TRANSVERSE WAKEFIELD EFFECT MEASUREMENT VIA MODEL-INDEPENDENT ANALYSIS *

John Irwin, Chun-xi Wang, Karl Bane, Yiton Yan, Michiko Minty, Franz J. Decker, Gennady Stupakov
Stanford Linear Accelerator Center, Stanford University, Stanford, CA 94309 USA

Abstract

Transverse wakefield effects due to structure misalignments can be an important source of emittance degradation in a linear collider. Though important, it is difficult to measure local wakefield effects and identify the sources. Recently, we have developed a novel method for analyzing the beam dynamics in an accelerator based on BPM readings, that is independent of any machine models. This method relies on, instead, statistically analyzing an ensemble of readings from a large number of BPMs and for a large number of pulses. In addition, pulse-by-pulse information of beam (and machine) parameters are used. By taking advantage of the spatial correlation and temporal structure of all these signals, such analysis allows observation of beam dynamics at a level well below the single BPM resolution as well as studies of subtle beam dynamics effects. Using this method, which is quick and non-invasive, we are able to measure the transverse wakefield effects due to structure misalignments in the SLC linac.

1 INTRODUCTION

A beam, when passing by a misaligned accelerator structure, will excite transverse wakefields that kick different parts of the beam by different amounts and therefore blow up the beam emmittance. Such a wakefield effect can be a major source of luminosity degradation in a linear collider. However, it is very difficult to measure transverse wakefield effects due to the weakness of the signals and the difficulty of separating such effects from other sources of perturbations. Using the current dependency of the wakefield, one can separate the wakefield effects from other effects. One idea is to measure beam orbits at different currents and then calculate the difference. Unfortunately, such measurements hardly succeed. One reason is the limited resolution in orbit measurements. More importantly, when beam current is changed, many other beam parameters (as well as the orbit) will be changed also. To avoid problems coming with current change, bunch length change has been used but with limited success. To illustrate this problem, Table 1 shows the correlations of current (bunch length) change with other beam parameters that we are able to monitor in the linac of Stanford Linear Collider (SLC). It was computed with 5000 electron pulses collected under normal running conditions. Clearly such correlations have to be taken into account in order to measure the wakefield effects correctly.

Table 1: Correlation coefficients of beam current and bunch length with other beam parameters

	current ΔI	bunch length σ_z
horizontal position x	-0.17	-0.52
horizontal angle x'	-0.03	-0.15
vertical position y	-0.08	0.01
vertical angle y'	0.10	0.20
long. beam phase	-0.48	-0.20
beam energy	-0.37	-0.18
bunch length	0.05	1
beam current	1	-0.05

Recently, a novel approach to analyze beam dynamics has been developed which we call "Model Independent Analysis (MIA)". It is a statistical analysis of BPM data and does not rely on any particular machine model. There are two major parts in MIA. One is noise reduction and degree-of-freedom analysis via singular value decomposition of a BPM-reading matrix. The other is a physical base decomposition of the BPM-reading matrix based on the time structure of beam (and machine) parameters. The combination of these two methods allows one to go below the resolution limit set by individual BPMs and to observe the beam dynamics at a much finer level. Physical base decomposition is particularly useful for understanding various beam dynamics issues, because it takes all known signal correlations into accounts. In the next section we describe MIA. Then, in the following section we apply MIA to obtain information about the structure misalignments in the SLC linac and their transverse wakefield effects.

2 MODEL INDEPENDENT ANALYSIS [1]

The transverse beam position of a pulse depends on various physical variables such as the initial conditions of the pulse, the settings of magnets, and the RF conditions. We can Taylor expand the beam position b over all variables as

$$b = b(\bar{x}_1, \bar{x}_1', \bar{\delta}, \bar{\sigma}_z, \cdots) + \sum_{v \in \{x_1, x_1', \cdots\}} \left. \frac{\partial b}{\partial v} \right|_{v = \bar{v}} \Delta v \quad (1)$$

$$+ \frac{1}{2} \sum_{v_1, v_2 \in \{x_1, x_1', \cdots\}} \left. \frac{\partial^2 b}{\partial v_2 \partial v_1} \right|_{\substack{v_1 = \bar{v}_1 \\ v_2 = \bar{v}_2}} \Delta v_1 \Delta v_2 + \cdots$$

where x_1, x_1', δ, σ_z are respectively initial beam position, angle, relative energy, and bunch length, given as examples of possible physical variables; the over bar indicates the expansion points; $\Delta v = v - \bar{v}$ and so on. The zero order term may have complicated dependency on the variables

and is sensitive to the unknown BPM offset errors. To get rid of it, we subtract the average over a large ensemble of pulses and study the difference

$$b - \langle b \rangle = \sum_v \left. \frac{\partial b}{\partial v} \right|_{v=\bar{v}} (\Delta v - \langle \Delta v \rangle) \qquad (2)$$

$$+ \frac{1}{2} \sum_{v_1, v_2} \left. \frac{\partial^2 b}{\partial v_2 \partial v_1} \right|_{\substack{v_1=\bar{v}_1 \\ v_2=\bar{v}_2}} (\Delta v_1 \Delta v_2 - \langle \Delta v_1 \Delta v_2 \rangle)$$

where $\langle \ \rangle$ indicates the average over an ensemble of pulses. Although we have found that some second derivatives (which characterize, e.g. the chromatic dependency of the betatron motion) may be significant at times, the third and higher order terms are generally negligible and will be dropped. We treat the first and second order terms on the same footing and rewrite Eq.(2) in a concise form:

$$b - \langle b \rangle = \sum_{\{q\}} q f_q \qquad (3)$$

where the variable $q = \frac{\Delta v - \langle \Delta v \rangle}{\mathrm{std}(\Delta v)}$ or $\frac{\Delta v_1 \Delta v_2 - \langle \Delta v_1 \Delta v_2 \rangle}{\mathrm{std}(\Delta v_1 \Delta v_2)}$ and f_q is the corresponding derivative $\left. \frac{\partial b}{\partial v} \right|_{\bar{v}} \cdot \mathrm{std}(\Delta v)$ or $\frac{1}{2} \left. \frac{\partial^2 b}{\partial v_2 \partial v_1} \right|_{\bar{v}_1, \bar{v}_2} \cdot \mathrm{std}(\Delta v_1 \Delta v_2)$. The physical variables are normalized by their standard deviations over the ensemble of pulses, so that all the q's are dimensionless and reflect the relative changes, while all the f's have the same dimension as the BPM readings.

For an ensemble of P pulses monitored with M BPMs, according to Eq.(3), the BPM-reading matrix B, consisting of $b - \langle b \rangle$, can be factorized as

$$B = QF^T + N \qquad (4)$$

where $Q_{P \times d} = [\vec{q}_1, \cdots, \vec{q}_d]$, $F_{M \times d} = [\vec{f}_1, \cdots, \vec{f}_d]$, and $N_{P \times M}$ contains the noise associated with each BPM reading. The column vector $\vec{q}_i$ contains the P values of the i-th physical variable and $\vec{f}_i$ contains the M components of the corresponding physical pattern. The q's are referred to as temporal patterns or time structures of the pulses, while the f's as spatial patterns or physical vectors. Note that the BPM-reading matrix B is the central object of MIA analysis. Eq.(4) is called the physical base decomposition.

We assume all the physical vectors are linearly independent, i.e. F has full column rank given by d. They form a complete basis for the row space of the BPM-reading matrix (i.e. range of B^T). Unlike P and M which can be chosen at will, dimension d is determined by the dynamics. One of the MIA achievements is to determine d. Generally, d is a small number and, we choose P and M so that $d \ll M \ll P$ to obtain statistical benefits. Typical numbers that we use are $d \sim 10$, $M \sim 10^2$, and $P \sim 10^3$. For convenience, we normalize B, Q, and N by $\sqrt{P}$, so that the important (variance-)covariance matrices of BPM readings and temporal patterns (q's) can be formed simply as $C_B = B^T B$ and $C_Q = Q^T Q$.

According to Eq.(3), a beam orbit is a linear combination of a limited number of "basic" orbits given by the f_qs.

In other words, the BPM reading pattern generated by each pulse is a superposition of certain basic patterns. This fact allows us to apply linear algebra concepts and matrix analysis techniques to the BPM data analysis. The statistical meaning of C_B and C_Q provides the connection between matrix analysis and statistical analysis.

Though SVD analysis of the BPM-reading matrix B (statistically, it is the principle components analysis of BPM readings) is a major aspect of MIA, it will not be described here due to space limitation. However this analysis is not crucial in the discussion of the wakefield effect measurements. What we will use is physical base decomposition of B using various kinds of pulse-by-pulse beam and machine parameters as tags –signals form a subset of the matrix Q. Mathematically, we know Q (or a subset of it) and B of Eq.(4), and need to solve for F. If we know all the physical variables with sufficient accuracy, the corresponding physical basis can be computed as

$$F^T = (Q^T Q)^{-1} Q^T B = C_Q^{-1} Q^T B \qquad (5)$$

and the errors due to noise are generally proportional to $\frac{1}{\sqrt{P}}$. The first expression reflects the least-squares fitting aspect of the solution, while the second expression emphasizes the importance of taking care of correlations among the observed variables.

The accuracy of Eq.(5) does not rely on the number of BPMs used. It simply fits each BPM reading to various temporal patterns individually and ignores any correlations among BPM readings. In fact, the BPM noise can be reduced statistically by taking into account the correlations among BPM readings. Therefore, if we cut the noise first and then apply Eq.(5), the noise level can potentially be reduced by a factor of $\frac{1}{\sqrt{M}}$, and we have

$$F^T = C_Q^{-1} Q^T U \underline{S} V^T + O(\frac{1}{\sqrt{P M}}) \qquad (6)$$

where USV^T is the SVD of B, and $\underline{S}$ indicates the zeroing of small singular values that are due to noise. This statistical error limit may be hard to achieve however due to problems such as machine instability and incomplete information in Q.

Usually we know only a subset of Q, say Q_s of $Q = [Q_s, Q_r]$. We can still calculate F_s according to Eq.(5) with Q_s, The error due to the missing part is

$$(F_s - F_s^{exact})^T = (Q_s^T Q_s)^{-1} Q_s^T Q_r F_r^T \qquad (7)$$

Therefore, if the known subset Q_s are uncorrelated with (orthogonal to) the remaining unknown temporal patterns, i.e. $Q_s^T Q_r = 0$, then we would obtain the same results as if we had measured all Q. Otherwise, the unknown part of the physical basis (i.e. F_r) will be mixed into the measured parts. This is the major limitation of this method.

3 TRANSVERSE WAKEFIELD EFFECT MEASUREMENT

Because of the detrimental effects of transverse wakefield due to structure misalignments, various methods [2, 3] have been used for the detection and correction of such wakefield effects. In the following, we present some preliminary results where MIA is used to measure the transverse wakefield effects. At the SLC, in addition to the beam transverse position, we can monitor beam current, bunch length, incoming beam (longitudinal) phase, and relative beam energy on a pulse-by-pulse basis. Other signals such as klystron phases along the linac have not been used in the present analysis. As is shown in Table 1, there are significant correlations among these signals, especially for the wakefield sensitive variables. MIA takes all known correlations into account, and therefore should provide a better measurement of the wakefield effects. To investigate this, we generated a 5 corrector, 1.2mm, local bump in the linac of SLC and measured its wakefield effect via MIA. We used readings from the beginning to about the 1/3 point of the linac (LI02–LI13), and collected 3 sets of 5000 pulses under the conditions: before the bump was applied (a), after it was applied (b), and after the bump was removed (c). Each set of data took a few minutes to collect.
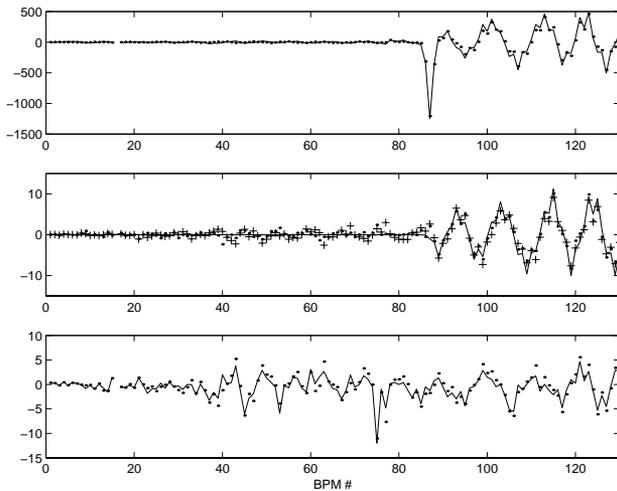
Figure 1: wakefield effect measurements in vertical plane

We applied MIA on all sets of data and then compared the vectors corresponding to the current jitter, and the results in y are shown in Figure 1 (all ordinate units are in μm). The top frame shows the differences of the averaged beam orbits. The solid line shows the difference between conditions b and a, while the dots are between conditions b and c. The corrector bump is clearly visible (it is not closed). The middle frame shows the difference of current vectors–the vectors correponding to current jitter. The dots are the differences between b and a, while the crosses are between b and c. The solid curve shows the calculated wakefield effect due to the bump. We see that the agreements are fairly good, especially when con-

sidering the fact that the BPM resolution is about 10 μm, which is as large as the signals. Furthermore, no external beam perturbation was used, and the signal is a rather weak 1.3% natural current jitter. As far as we know, such accurate transverse wakefield effect measurements in a linac are unprecedented. Note that the errors are on the order of a few microns, which is much larger than the statistical limit. Therefore, it is still possible to further improve both measurement and analysis. Frames 1 and 2 demonstrate that the current vectors obtained via Eq.(5) are correct. The bottom frame shows the current vectors of conditions a and c, which are the wakefield effects due to misalignments (and corrector offsets, etc.) in the normal running machine. An immediate application of such current vectors is the detection of structure misalignments and confirmation of wakefield calculations.

We performed a similar analysis in x also. We found that, one set of results agrees with the calculation while another has much larger deviations. The discrepancy in the horizontal cases may be due to some unknown jitter sources that are correlated with the current. We repeated these experiments several weeks later and obtained similar results in both the vertical and horizontal planes.

Our measurement results are still preliminary because limited machine time prevented us from thorough investigation. Nonetheless, they are very encouraging and promising. Since such measurements need not perturb the beam, they are basically non-invasive to normal machine operation and in principle can be done parasitically and quickly after the method matures. On the other hand, intentionally introduced larger current variation will improve the sensitivity to the misalignments. This method can potentially become a powerful tool for finding structure misalignments.

4 ACKNOWLEDGMENTS

5 REFERENCES

[1] A comprehensive documentation of MIA will soon be published under the title "Model independent analysis of beam dynamics in accelerators"

[2] T.O. Raubenheimer, K. Kubo, "A technique for measuring and correcting emittance dilutions due to accelerator structure misalignments," NIM A370, p. 303-311

[3] F.-J. Decker, et al., "Super-ASSET: a technique for measuring and correcting accelerator structure misalignments at the SLC," Proceedings of PAC97